

Study of Thermal Decomposition Kinetics of Palm Oleic Acid-Based Alkyds and Effect of Oil Length on Thermal Stability

Shahla Ataei · Rosiyah Yahya · Seng Neon Gan · Aziz Hassan

Published online: 24 December 2011
© Springer Science+Business Media, LLC 2011

Abstract Thermal decomposition kinetics of three palm oleic acid-based alkyds with different oil lengths and having different molecular weights were studied using TGA measurements under non-isothermal conditions. Activation energies were obtained from Kissinger and Ozawa, Flynn and Wall (OFW) methods and subsequently the pre-exponential factor, A , degradation rate constant, k , for all the alkyds were also determined. From kinetic analysis of the thermal decomposition using the OFW method, it was found that degradation of all the alkyds has taken place in more than two stages, corresponding to different mechanisms. As shown from Ozawa and Kissinger methods, the chemical composition of the alkyds influenced the thermal degradation; increasing the phthalic anhydride and glycerol, and decreasing the oleic acid increased the thermal stabilities of the alkyds.

Keywords Thermal decomposition · Non-isothermal · Oleic acid · Oil length · Activation energy

Introduction

Polymers have different stabilities and thus the qualitative fingerprint afforded by TG–DTG in terms of temperature range, extent and kinetics of decomposition provides a rapid means to distinguish one polymer to another using only small amount of materials.

Green unsaturated polyesters such as alkyds are important renewable and environmentally friendly polymers and

have attracted considerable attention in the last decades. Alkyd resins, being in this category, are important area in the industry, as one can just design alkyds by changing the oil length and subjected them to suitable physical or chemical modifications for various potential applications such as surface coating, adhesive, printing ink, fibers and temperature resistant performance materials pneumatic tire and so on [1–7]. However, some health problems may arise from thermal decomposition of the materials due to evolution of some toxic products.

Throughout the literature, there are many papers concerning the synthesis and characterization of various new high performance polymers with much interest on thermal stability study of the polymers. However, based on our literature search, for alkyds only a few amount of work has been published on the thermal behavior of alkyds and also their thermal decomposition kinetic analysis [8–10].

The kinetic parameters of polymers can provide important additional information for their use and process ability as new materials. In the determination of kinetic parameters, the non-isothermal methods have been used extensively. Many authors have employed different computational methods, among which are the Freeman-Carroll [11], Coats-Redfern [12], Doyle [13] modified by Zsako [14], Kissinger [15] and Ozawa, Flynn and Wall (OFW) [16, 17].

With the advent of new instrumentation, the recognition of products resulting from thermal decomposition can be identified. Various works [18, 19] have demonstrated the contribution of the techniques coupled with systems such as TG/DTA-MS, TG/DTA-FTIR and TG/DTA-GC/MS. These coupled methods supply structural information and can further clarify the decomposition process. The TG-GC-MS coupled system is an individual technique that provides a direct measurement of weight loss and separates the products.

S. Ataei · R. Yahya (✉) · S. N. Gan · A. Hassan
Department of Chemistry, University of Malaya,
50603 Kuala Lumpur, Malaysia
e-mail: rosiyah@um.edu.my

In this work, kinetics of non-isothermal decomposition for three palm oleic acid-based alkyds were studied by TGA. The purpose of this work is to examine in more detail the thermal decomposition and to understand the effect of the oleic acid content (oil length) on the complexity of the decomposition mechanism in different alkyds. The Kissinger and OFW methods were employed to obtain the kinetic parameters for this purpose. Thermal decomposition of evolved toxic products of alkyds at their maximum rate of decomposition temperature was also analyzed and identified using TG-GC-MS coupled technique.

Experimental

Materials

The alkyds used in this work were synthesized following the procedure reported earlier [20]. The molecular structure of the alkyds under investigation had been varied by using 28, 40 and 65 wt% of oleic acid in the overall formulation and labelled as AlkOA28 (short oil length), AlkOA40 (medium oil length) and AlkOA65 (long oil length) respectively. Details of these alkyds as per formulation are given in Table 1.

Determination of Kinetic Parameters for Thermal Decomposition of Alkyds and Decomposition Products

Alkyd samples were analyzed by Perkin Elmer TGA model 6 instrument and the measurements were done using about 16 ± 1 mg of sample, under nitrogen atmosphere flow rate of 20 mL min^{-1} from 30 to $900 \text{ }^\circ\text{C}$. The heating rates were 10, 15, 20, 25 and $30 \text{ }^\circ\text{C min}^{-1}$.

The decomposition kinetics of alkyds were studied using two methods through TGA. The activation energy of decomposition can be estimated via the Kissinger equation (1),

$$-\ln \left(q/T_p^2 \right) = E_d/RT_p - \ln (AR/E_d) \quad (1)$$

Table 1 Formulation and physico-chemical properties of the alkyds

| Compositions/ properties | AlkOA28 | AlkOA40 | AlkOA65 |
|---|--------------------------|----------|-------------------|
| Oleic acid (%) | 28 | 40 | 65 |
| PA (%) | 44 | 34 | 15 |
| Glycerol (%) | 28 | 26 | 20 |
| Color | Dark viscous brownish | Brownish | Light brownish |
| Acid value (mg KOH g ⁻¹) | 16 | 16 | 8 |
| Molecular weight (M _n) | 2,070 | 1,210 | 980 |

where q is the heating rate, T_p refers to the temperature at maximum rate of decomposition where peak deflection occurs in the DTG curves, R universal gas constant ($8.3143 \text{ J K}^{-1} \text{ mol}^{-1}$) and, A the pre-exponential factor and E_d decomposition activation energy. E_d for each alkyd was calculated from the slope of the straight line of $-\ln (q/T_p^2)$ versus $1/T_p$.

Degradation rate constant, K , at T_p was also calculated using Eq. 2.

$$K = A \exp^{-E_d/RT_p} \quad (2)$$

Another method to obtain decomposition activation energy is the iso-conventional method of OFW. This method includes the measuring of the temperatures corresponding to fixed values of conversion (α) from experiments at different heating rates, q . The graph, $\ln (q)$ versus $1/T$ from Eq. 3 is used to construct the Ozawa plot,

$$\ln (q) = \ln \left[\frac{Af(\alpha)}{dx/dT} \right] - \frac{E_d}{RT} \quad (3)$$

where q is the heating rate, T is the temperature from the various heating rates at the same loss weight, E_d the activation energy and R the universal gas constant. According to the Eq. 3, Ozawa plot should give straight line and its slope is proportional to the activation energy ($-E_d/R$). The OFW method is a method which assumes that conversion function $f(\alpha)$ does not change with the alteration of the heating rate for all values of α . If the determined activation energy is the same for the various values of α , the existence of a single-step reaction can be concluded. While, a change of E_d with increasing degree of conversion is an indication of a complex reaction mechanism that invalidates the separation of variables involved in the OFW analysis [21].

A sequence of experiments was carried out for AlkOA28 and AlkOA65 using TG-GC-MS system to identify decomposition products. Heating rate in TGA was $20 \text{ }^\circ\text{C min}^{-1}$. Evolved gases of these two samples were collected at specified temperature (at maximum rate of decomposition temperature) as this temperature was $385 \text{ }^\circ\text{C}$ for AlkOA28 and $418 \text{ }^\circ\text{C}$ for AlkOA65 and subsequently separated in the gas chromatograph with column Elite DB5. Evolved gas analysis was accomplished using Clarus 600 GC/MS instrument connected through the TL 9000 heated transfer line interface under helium atmosphere. The mass spectrometer was operated in the electron bombardment ionization (70 eV) mode and the m/z range of 50–300 amu.

Results and Discussion

Thermal Stability and Kinetic Parameters of Alkyds

Thermal decomposition of three alkyds was studied by determining their mass loss during heating. TG and DTG

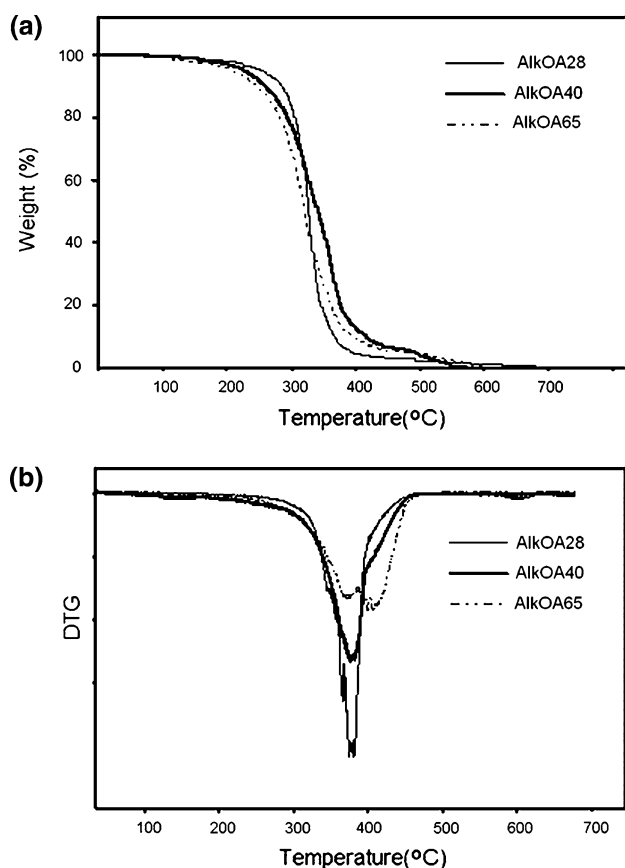


Fig. 1 a TG and b DTG curves of three alkyds at heating rate 10 °C/min

curves at heating rate 10 °C min⁻¹ for the three alkyds are presented in Fig. 1a, b respectively. From these thermograms, it can be seen that AlkOA28 has a relatively higher thermal stability, followed by AlkOA40 and AlkOA65.

Looking at DTG curves of AlkOA28 at different heating rates (Fig. 2a), it is clear that the peak temperature, T_p , shifts to higher values with increasing the heating rate.

Similar trends are observed for both AlkOA40 and AlkOA65 using DTG thermograms (Fig. 2b, c); an increment of 17 °C for AlkOA28, 20 °C for AlkOA40 and 26 °C for AlkOA65 (Table 2).

To further analyze the degradation mechanisms of the alkyds it is important that the kinetic parameters such as activation energy E_d , pre-exponential factor A and degradation rate constant, k be evaluated. The plots of $-\ln(q/T_p^2)$ against $1/T_p$ using Eq. 1 for three samples are shown in Fig. 3.

From the calculated activation energies in Table 2, an improvement in the thermal stability of the samples can be seen with increase in PA and glycerol as AlkOA28 shows relatively the highest thermal stability due to the highest activation energy followed by AlkOA40 and AlkOA65. The trend in thermal stability of the alkyds may also be due to enhancement of the intermolecular attraction among the

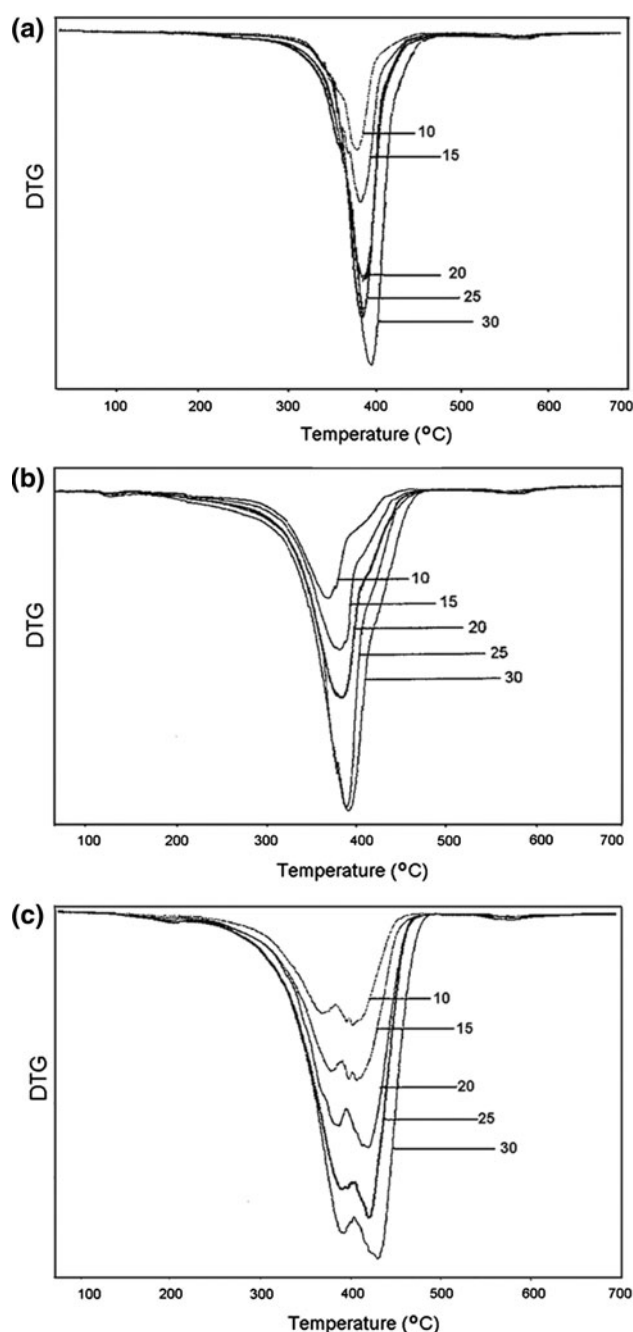
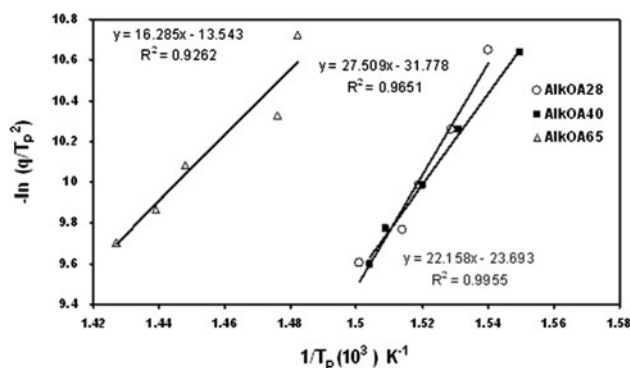


Fig. 2 DTG thermograms of a AlkOA28, b AlkOA40, c AlkOA65 at various heating rates

polymer chains. The increasing number of –OH groups in the alkyd formulation and the formation of hydrogen bonds between –OH groups may have effect on increasing the thermal stability. The improved thermal stability can also be explained through the reduced mobility of the polymer chains in the polyesters. PA having rigid structure can usually hinder the motion of the polymer chains. During thermal decomposition of samples, relatively weak bonds break at lower temperature whereas the stronger bonds in

Table 2 Kinetic analysis data of alkyds at different heating rates using Kissinger plots

| Alkyd code | q (K min ⁻¹) | T_p (K) | A (s ⁻¹) | E_d (kJ mol ⁻¹) | Average A (s ⁻¹) | k (s ⁻¹) | Average (k) |
|------------|----------------------------|-----------|------------------------|-------------------------------|--------------------------------|------------------------|-----------------|
| AlkOA28 | 10 | 649.44 | 2.78×10^{16} | 229.0 | 2.99×10^{16} | 0.011 | 0.021 |
| | 15 | 653.90 | 3.08×10^{16} | | | 0.016 | |
| | 20 | 658.35 | 3.04×10^{16} | | | 0.021 | |
| | 25 | 660.41 | 3.32×10^{16} | | | 0.026 | |
| | 30 | 666.28 | 2.71×10^{16} | | | 0.031 | |
| AlkOA40 | 10 | 644.98 | 5.88×10^{12} | 183.0 | 5.73×10^{12} | 0.009 | 0.017 |
| | 15 | 653.35 | 5.55×10^{12} | | | 0.013 | |
| | 20 | 658.05 | 5.73×10^{12} | | | 0.017 | |
| | 25 | 662.76 | 5.57×10^{12} | | | 0.021 | |
| | 30 | 665.11 | 5.90×10^{12} | | | 0.025 | |
| AlkOA65 | 10 | 674.59 | 1.40×10^8 | 134.0 | 1.61×10^8 | 0.006 | 0.011 |
| | 15 | 677.29 | 1.89×10^8 | | | 0.009 | |
| | 20 | 690.66 | 1.53×10^8 | | | 0.011 | |
| | 25 | 695.11 | 1.63×10^8 | | | 0.014 | |
| | 30 | 700.68 | 1.60×10^8 | | | 0.016 | |

**Fig. 3** Kissinger plots for the three alkyds

the aromatic rings take place at higher temperature [22]. As the tendency for chain scission is higher in the samples with higher number of methylene groups [23], the oleic acid, due to its long chain is more thermally labile and thus decreases the thermal stability. It is well known that differences in the molecular weights may also affect the thermal decomposition behavior of polymers [24]. The synergy of all these reasons has significant contribution to the increment of the thermal stability of AlkOA28.

Using the Arrhenius equation (2), the calculated degradation rate constant, k , at T_p , as shown in Table 2, shifts to higher values with increasing the heating rate.

Kinetic Analysis Alkyds with Different Oil Lengths Using OFW Method

Alkyds with different oil lengths have different chemical structure; short oil length alkyd shows resin-like properties (with less branching) while long oil-length alkyd indicates oil-like properties (with more branching) [25].

Using OFW equation (3), relationship between activation energy and degree of conversion (α) in decomposition reactions of the alkyds can be clarified. Some of the Ozawa plots for AlkOA28 are displayed in Fig. 4a.

From DTG thermograms of AlkOA28 (Fig. 2a), it is clear that the mass loss follows at least two stages under all heating rates. The first is in the temperature region between 376 and 394 °C and the second is before 700 °C. Therefore, for the precise kinetic description of mass loss, at least two different mechanisms have to be considered. However, in OFW method, the equation used is derived assuming constant activation energy, introducing systematic error in the estimation of E_d [26]. Thus, the dependence of E_d on α value, as calculated with OFW method, can be separated into three regions corresponding to at least three different mechanisms and each one mechanism presents different activation energy (Fig. 5).

The E_d s corresponding to various conversion of decomposition reaction were quantified in Table 3 whereby, the first is for values of α up to 0.3, in which E_d presents an important increase, the second ($0.3 < \alpha < 0.7$) in which E_d presents no important increase and in the third region for $0.7 < \alpha < 0.9$ in which E_d again shows a significant increase.

In the case of alkyds AlkOA40 and AlkOA65, the DTG curves at different heating rates (Fig. 2b, c) show mass losses occurring in 3 and 4 stages under all heating rates. For AlkOA40, the first stage is the temperature region close to the 135 °C, the second around 371–392 °C and the third step is before 700 °C. The Ozawa plots for AlkOA40 between 10 and 90% weight losses are displayed in Fig. 4b. The results as shown in Fig. 5 reveal that the dependence of E_d on α value can be divided into four distinct regions as summarized in Table 3. The first is for values of α up to

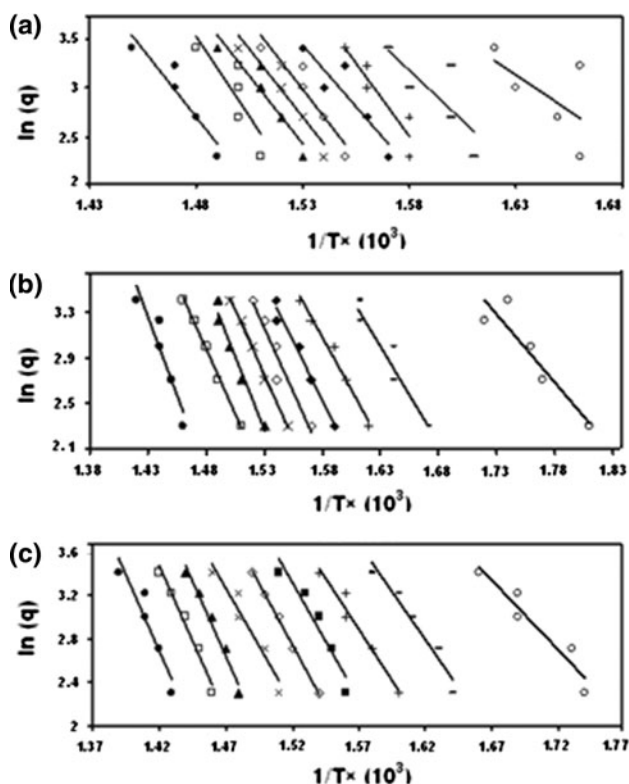


Fig. 4 Ozawa plots of **a** AlkOA28, **b** AlkOA40 and **c** AlkOA65 at various conversions of reaction: $\alpha = 0.1$ (open circle), $\alpha = 0.2$ (minus sign), $\alpha = 0.3$ (plus sign), $\alpha = 0.4$ (closed diamond), $\alpha = 0.5$ (open diamond), $\alpha = 0.6$ (multiple sign), $\alpha = 0.7$ (closed triangle), $\alpha = 0.8$ (open square), $\alpha = 0.9$ (closed dot)

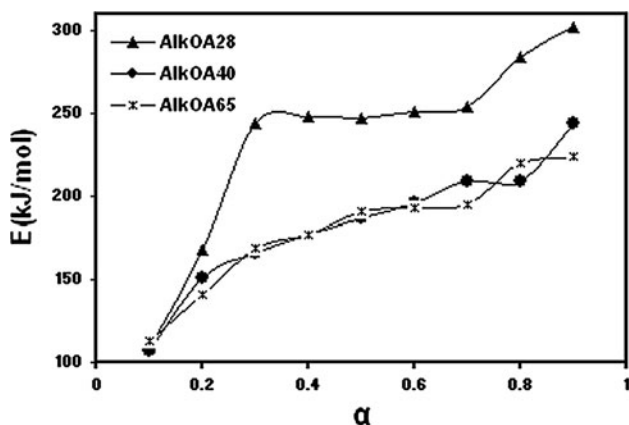


Fig. 5 Activation energies corresponding to fixed values of α using Ozawa plots of AlkOA28 (closed triangle), AlkOA40 (closed dot) and AlkOA65 (multiple sign)

0.2, in which E_d presents a significant increase, the second for values between $0.2 < \alpha < 0.7$ in which E_d shows a slight monotonous increase, the third region appears between $0.7 < \alpha < 0.8$ in which E_d shows no increase and the fourth region can be seen for $\alpha > 0.8$ whereby E_d displays an important increase. The activation energies for

Table 3 Calculated E_d using the OFW method at various conversions of decomposition reaction under different heating rates for the alkyds

| Conversion (α) | E_d (kJ/mol) | | |
|-------------------------|----------------|---------|---------|
| | AlkOA28 | AlkOA40 | AlkOA65 |
| 0.1 | 109.6 | 107.0 | 105.8 |
| 0.2 | 168.3 | 151.3 | 141.5 |
| 0.3 | 243.9 | 165.4 | 169.0 |
| 0.4 | 247.9 | 176.6 | 177.3 |
| 0.5 | 247.5 | 187.1 | 191.5 |
| 0.6 | 252.6 | 195.6 | 192.7 |
| 0.7 | 254.4 | 208.6 | 194.8 |
| 0.8 | 284.1 | 209.2 | 219.8 |
| 0.9 | 302.1 | 243.6 | 224.4 |

this sample are very small at the initial stage of decomposition and higher at the final stage. These initial lower values are most likely associated with initiation process that corresponded to volatilization of small molecules or carbon dioxide produced from chain ends [23]. By increasing the temperature, random scission of macromolecular chains predominates [24].

For AlkOA65, first stage of decomposition is between 100 and 200 °C, second around 369 °C, third step is between 400 and 428 °C and final stage takes place before 700 °C. The Ozawa plots for AlkOA65 are shown in Fig. 4c. From Table 3 and slopes obtained in Fig. 5, the degradation process can be separated into five regions. The initial stage of decomposition that occurs up to $\alpha < 0.3$ shows an important increase in activation energy, the second stage appears at $0.3 < \alpha < 0.5$ in which E_d demonstrates a small increment, the third region at $0.5 < \alpha < 0.7$ displays no increase in E_d , the fourth stage of decomposition appears at $0.7 < \alpha < 0.8$ having a big increase in activation energy and the final region for $\alpha > 0.8$ in which E_d exhibits a slight increase again.

By using OFW method, decreasing the molecular weight of alkyd reveals more complexity in decomposition reaction and all results are consistent with the presence of overlapped peaks in DTG curves.

GC–MS Analysis

Evolved gases of AlkOA28 and AlkOA65 (samples with short and long oil lengths respectively), were analysed using GC–MS spectrometer at maximum rate of decomposition temperature. Although the GC–MS spectra seem to be complex due to many mass fragmentation ions brought by the various decomposed gases, the significant observed mass peaks do give important information. Comparing the mass spectra of the decomposition products (Fig. 6), it is observed that the decomposition patterns are

Fig. 6 Mass spectra of decomposition products for **a** AlkOA28 at 385 °C and **b** AlkOA65 at 418 °C

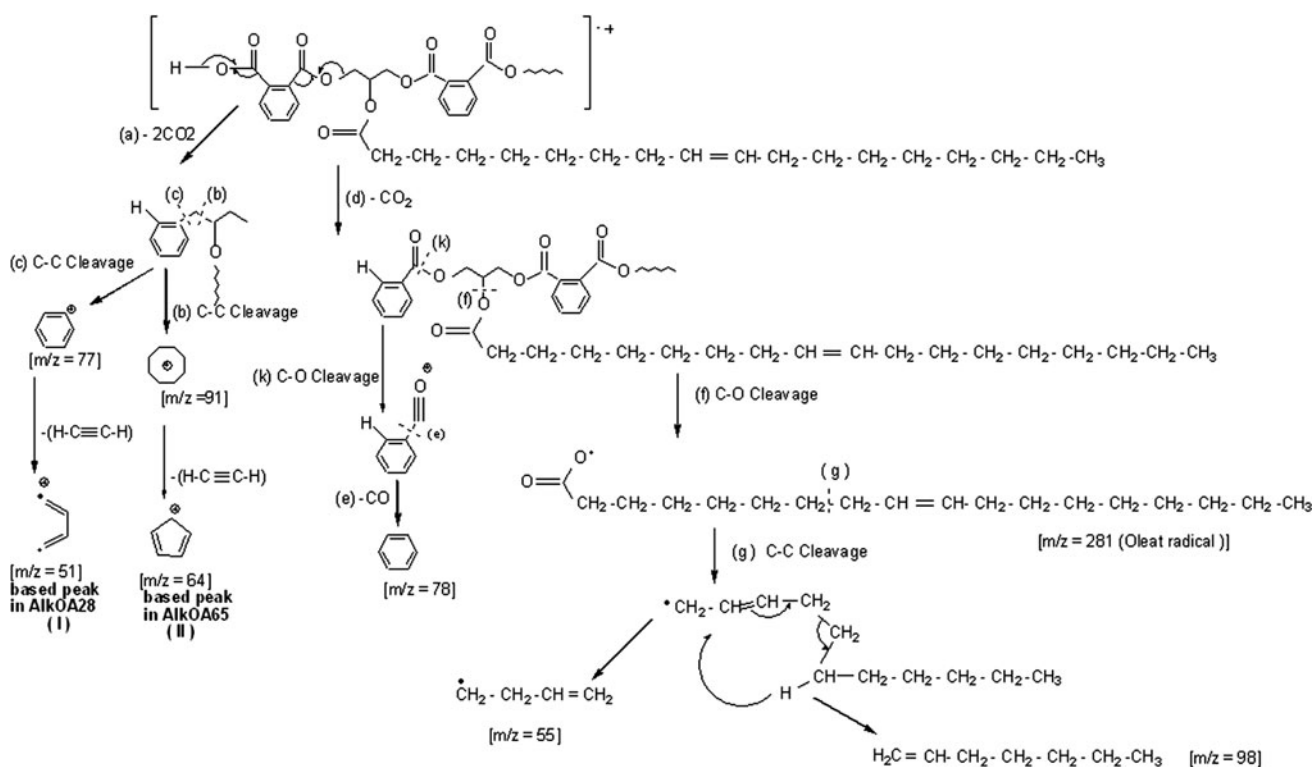
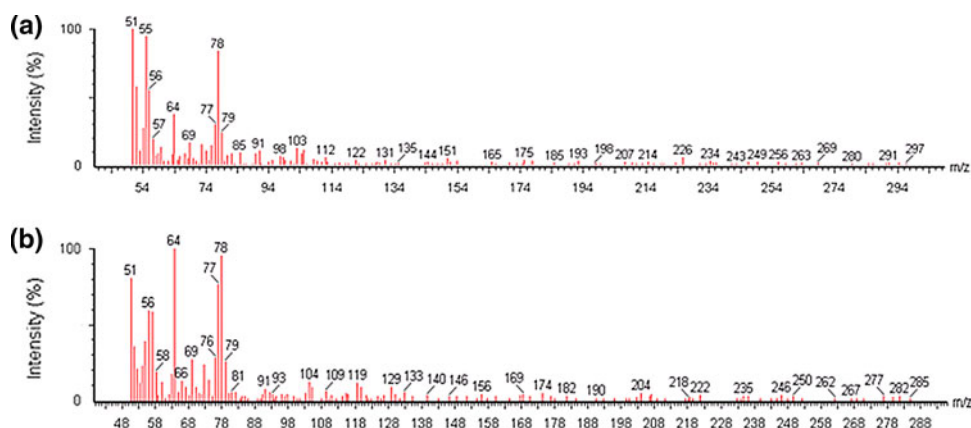


Fig. 7 Possible mechanism involved in decomposition reactions of AlkOA28 and AlkOA65

almost the same. The signal at m/z 78 could be due to benzene ring from PA, while signals at 281 and 282 with very low intensity can support existence of oleic acid indicating that it was almost completely decomposed. Also, the set of $m/z = 57, 73, 89$ ions observed with low intensity are from glycerol. PA and oleic acid and glycerol are starting materials for the alkyds. Mass spectra show base peaks of highest intensity at m/z values of 51 (for AlkOA28) and 64 (for AlkOA65) which can be attributed to 1,3-butadiene diradical carbocation (I) and cyclopentadiene carbocation (II) respectively. The presence of these peaks proposes the possible cleavages as given in Fig. 7.

Conclusion

The kinetic parameters of the three palm oleic acid-based alkyds containing different percentages of oleic acid have been investigated using TGA. Based on Kissinger method, the activation energies for the alkyds AlkOA65, AlkOA40 and AlkOA28 are found to be 134, 183 and 229 kJ mol^{-1} respectively. The OFW method reveals more complexity in the degradation reactions with decrease in the molecular weight of the alkyds. Irrespective of the methods used, the thermal properties of the alkyd improve as the PA/oleic acid ratio is increased from 0.22 in AlkOA65 to 1.55 in

AlkOA28 and glycerol/oleic acid ratio raised up from 0.32 in AlkOA65 to 1 in AlkOA28. The gaseous species produced from AlkOA28 and AlkOA65 as analyzed by TG-GC-MS showed presence of benzene arising from PA, as significant intensity, among the products of decomposition for both the alkyds. In addition, this study suggests the use of the technique, i.e., separation and identification of the volatile products recorded in the TG-GC-MS coupled system, as a screening procedure for alkyd composition which is an important area in both the industry and environment.

Acknowledgments The authors would like to thank the University of Malaya for financial support under grant no. PS380/2009B.

References

1. Heiskanen N, Jamsa S, Paajanen L, Koskimies S (2010) *Prog Org Coat* 67:329
2. Packham DE (2009) *Int J Adhes Adhes* 29:248
3. Ataei S, Yahya R, Gan SN (2011) *Prog Org Coat* 72:703
4. Hattori T, Terakawa K, Ichikawa N, Sakaki T, Choong DH, Gan SN, Lee SY (2007) US Patent, US 2007/0100061A1, Joint Patent of UM& SRI; pp 3–5
5. Lee SY, Gan SN, Hassan A, Terakawa K, Hattori T, Ichikawa N, Choong DH (2011) *J Appl Polym Sci* 120:1503
6. Velayutham TS, Abd Majid WH, Ahmad AB, Gan YK, Gan SN (2009) *J Appl Polym Sci* 112:3554
7. Velayutham TS, Abd Majid WH, Ahmad AB, Gan KY, Gan SN (2009) *Prog Org Coat* 66:367
8. Amaral GCA, Crespi MS, Ribeiro CA, Hikosaka MY, Guinesi LS, Santos AF (2005) *J Therm Anal Calorim* 79:375
9. Dias DS, Crespi MS, Ribeiro CA, Fernandes JLS, Cerqueira HMG (2008) *J Therm Anal Calorim* 91:409
10. Dias DS, Crespi MS, Ribeiro CA (2008) *J Therm Anal Calorim* 94:539
11. Freeman ES, Carroll B (1958) *J Phys Chem* 62:394
12. Coats AW, Redfern JP (1964) *Nature* 201:68
13. Doyle CD (1961) *J Appl Polym Sci* 15:285
14. Zsako J (1968) *J Phys Chem* 72:2406
15. Kissinger HE (1957) *Anal Chem* 29:1702
16. Ozawa TB (1965) *Bull Chem Soc Jpn* 38:188
17. Flynn J, Wall LA (1966) *Polym Lett* 4:232
18. Parra DF, Mercuri LP, Matos JR, Brito HF, Romano RR (2002) *Thermo Chim Acta* 386:143
19. Zhang P, Wu L, Li BG (2009) *Polym Degrad Stab* 94:1261
20. Ataei S, Yahya R, Gan SN (2011) *J Polym Environ* 19:540
21. Ozawa T (1970) *J Therm Anal Calorim* 2:301
22. Ferdous D, Dalai AK, Bej SK, Thring RW (2002) *Energy Fuels* 16:1405
23. Chrissafis K, Paraskevopoulos KM, Bikiaris DN (2005) *Thermo Chim Acta* 435:142
24. Chrissafis K, Paraskevopoulos KM, Bikiaris DN (2006) *Thermo Chim Acta* 440:166
25. Patton TC (1962) *Alkyd resin technology*. Interscience publisher, Wiley, New York
26. Vyazovkin S (2002) *Int J Chem Kinet* 34:418